

Model Estimates of Global Carbon Flux between Vegetation and the Atmosphere^①

Li Yinpeng (李银鹏) and Ji Jinjun (季劲钧)

Institute of Atmospheric Physics, Chinese Academy of Sciences, Beijing 100029

(Received September 1, 2000)

ABSTRACT

The net primary productivity (NPP) of global terrestrial vegetation is estimated by an Atmosphere–Vegetation Interaction Model (AVIM). AVIM consists of two intercoupled components: physical processes, involving water and energy transfer among soil, vegetation and the atmosphere at the land surface and eco–physiological processes, i.e. photosynthesis, respiration, dry matter allocation, littering, phenology. Globally vegetation is classified into 13 types and soil texture is classified into 6 types. The estimated NPP for different vegetation types at 1637 sites are validated with the observed data provided by EMDI. The main results of NPP estimation show that global averaged NPP is $405.13 \text{ g C m}^{-2}\text{yr}^{-1}$, varying from $99.58 \text{ g C m}^{-2}\text{yr}^{-1}$ (tundra) to $996.2 \text{ g m}^{-2}\text{yr}^{-1}$ (rainforest). Global total annual NPP is about $60.72 \text{ Gt C yr}^{-1}$, in which the maximum part, about $15.84 \text{ Gt C yr}^{-1}$, accounting for 26.09% of the total is contributed by tropical rainforest. The maximum carbon sink occurs in the temperate region of the Northern Hemisphere. The global spatial and seasonal distribution of terrestrial NPP is estimated reasonably.

Key word: Carbon flux, Net primary productivity (NPP), Terrestrial ecosystem, Atmosphere–vegetation interaction

1. Introduction

Carbon dioxide is an important greenhouse gas in the atmosphere. The CO_2 concentration in the atmosphere has increased from 280 ppm in the 1750's to 367 ppm in 1999 (IPCC, 2001), mainly due to burning of fossil fuel. In nature the oceans, terrestrial ecosystem and the atmosphere are three main carbon pools in carbon biogeochemical cycle. The ocean is the largest carbon pool. The carbon storage in deep ocean is about $4 \times 10^4 \text{ Gt}$ (10^{15} gram), 720–765 Gt in the atmosphere and 2200 Gt in terrestrial ecosystem, in which 600 Gt in vegetation and 1200 Gt in soil. Current annual CO_2 release to the atmosphere by fossil fuel burning is approximately (5.4–6.3) Gt (IPCC, 2001). The annual CO_2 exchange between ecosystem and the atmosphere is about 120 Gt. That is to say a small fluctuation of air–land CO_2 flux, for example 5%, would be equal to or excess the CO_2 emission by human activities. This is exactly because of the important role of carbon cycle in global environment change, carbon cycle becomes a critical issue in the International Geosphere and Biosphere Program (IGBP) in the present and in the future.

The carbon exchange between ecosystem and the atmosphere, i.e. the net primary productivity (NPP) has long been studied since the 1970's. Lieth (1975) estimated the global NPP distribution with the empirical formula which links directly NPP to climatic conditions (temperature or precipitation). In the past few years a comparison project aimed at simulation of

^①This study was supported by National Key Basic Research Development Program (G1999043400).

global NPP distribution was carried out, over 10 models involving dynamical ecosystem model, biogeochemical process model and empirical model participated (Cramer et al., 1999). More recently the Ecosystem Model / Data Inter-comparison project (EMDI) has been initiated under the support of GAIM, a task force of IGBP (Sahagian, 2000). The attempt of this study is to estimate quantitatively carbon exchange between the atmosphere and terrestrial ecosystem with an Atmosphere-Vegetation Interaction Model (AVIM). In section 2, the structure of AVIM and datasets used are introduced. In section 3, the simulated global NPP is analysed and the summary will be given in Section 4.

2. AVIM structure and related data bases

2.1 Brief description of AVIM

AVIM (Ji, 1995), an atmosphere-vegetation two way interaction model, is constructed on the basis of the following mechanism: The physical processes involving the transient materials (water, CO₂) and energy (radiation, sensible and latent heat) exchanges between land surface and abiotic environment (atmosphere, soil). And thermal and humid states at the land surface affect the plant physiological growth processes, and lead to plant macro-morphological changes (canopy height, leaf area index, etc.), and then the changes of surface dynamical and physical parameters, in turn influence the physical exchange processes between soil, vegetation and the atmosphere. AVIM has been used to simulate physical and physiological processes at the sites of temperate mixed forest (Ji, 1995), crops (Ji and Hu, 1999), grassland (Ji and Yu, 1999) and for regional issues e.g. Northeast China Transect (NECT) and Tibet (Lu, 1999). In this paper we would generalise AVIM to global terrestrial ecosystem.

The structure of AVIM is shown in Fig. 1 (Ji, 1995). From upper to lower part there are three layers: the atmosphere, canopy and soil. The left side of the system displays the physical processes that construct the Land surface Process Model (LPM) (Ji and Hu, 1989). The right side of the system displays the plant physiological processes. The canopy is assumed to be a horizontal homogeneous layer with the coverage σ_f . The soil is divided into N layers. The climatic conditions of the bottom layer are assumed to be constant. In the following the brief description of model will be shown.

2.1.1 Physical transport processes

The changes of canopy temperature T_f and liquid water (or snow) M_f are governed by energy and water conservation equations

$$C_f \cdot \frac{dT_f}{dt} = R_{nf} - H_f - LE_f, \quad (1)$$

$$\frac{dM_f}{dt} = P_f - D_f - \frac{1}{\rho_w} \cdot E_w. \quad (2)$$

The subscript 'f' denotes the variables related to canopy. Here C_f is heat content of canopy, which is proportional to leaf area index (LAI). R_{nf} , H_f and E_f stand for net radiation, sensible and latent heat fluxes of canopy respectively. P_f , D_f and E_w are the intercepted precipitation, drainage of canopy and evaporation from the wet part of foliage. ρ_w is the density of water. The equations of soil temperature and moisture for each layer can be written as

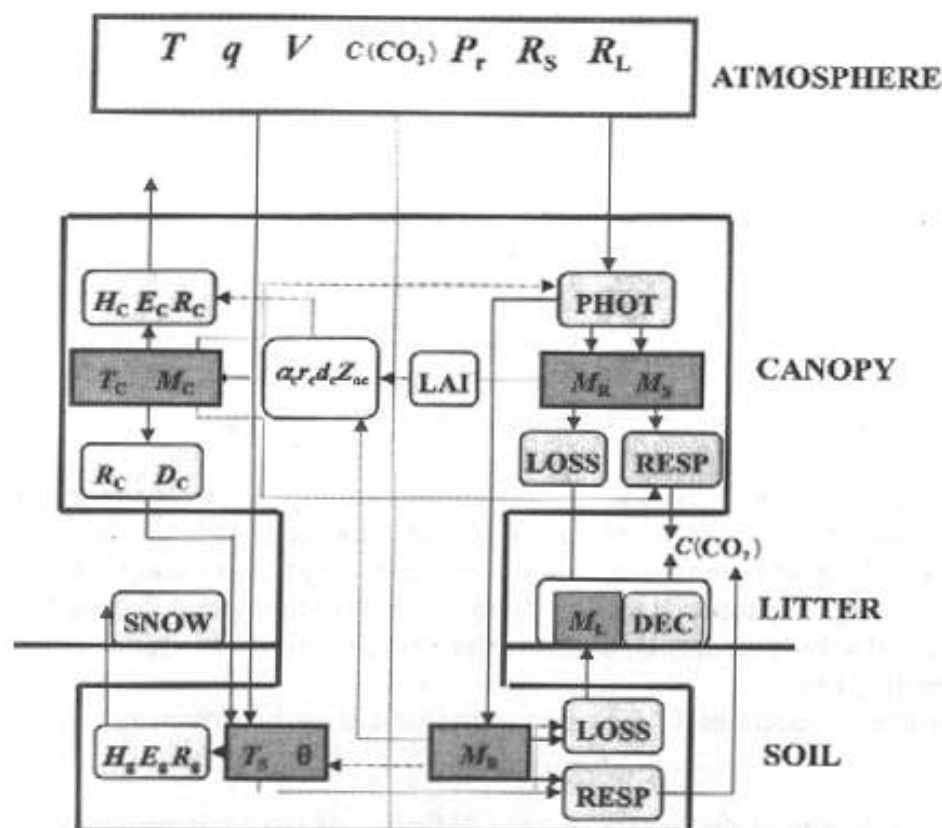


Fig. 1. Schematic structure of the Atmosphere-Vegetation Interaction Model (AVIM). The physical processes are displayed on the left side and plant eco-physiological processes on the right side. The solid lines show the flows of energy and materials and the dashed lines show the interaction directions. The atmospheric variables $T, q, V, C(\text{CO}_2), P_r, R_s$, and R_L are the temperature, specific humidity, wind speed, carbon dioxide concentration, precipitation, short wave and long wave radiation, respectively. The physical variables T_c, M_c, T_s , and θ are the canopy temperature and water content, soil temperature and moisture. M_p, M_s, M_r , and M_L are the biomass for leaf, stem, root and litter dead matter. The symbols 'PHOT', 'LOSS', 'RESP', and 'DEC' denote the processes of photosynthesis, loss, respiration and decomposition of dry matter. H, E , and R stand for the sensible latent heat, evaporation (or transpiration) exchanges and radiative transfer processes. The subscript 'c' represent the processes for canopy and 's' for the soil. 'SNOW' stands for snow cover, 'LAI' for leaf area index, and α_r, r_s, d, Z_{0c} for albedo, stomatal resistance, zero plane displacement and roughness, respectively (Redraw from Ji, 1995).

$$\frac{\partial T_i}{\partial t} = \frac{1}{(\rho C d)_i} \cdot \left[\lambda_{i+1,i}(W) \cdot \left(\frac{\partial T}{\partial z} \right)_{i+1,i} \lambda_{i+1,i} - \lambda_{i,i-1}(W) \cdot \left(\frac{\partial T}{\partial z} \right)_{i,i-1} \right], \quad (3)$$

$$\frac{\partial W_i}{\partial t} = \frac{1}{d_i} \left[D_{i+1,i}(W) \cdot \left(\frac{\partial W}{\partial z} \right)_{i+1,i} - D_{i,i-1}(W) \cdot \left(\frac{\partial W}{\partial z} \right)_{i,i-1} \right] + \frac{\partial K_w}{\partial z} - S_w, \quad (4)$$

where T_i and W_i are soil temperature and moisture for layer i , and $W \equiv \theta / \theta_s$, where θ, θ_s are the volumetric moisture content and its saturated value, i.e. porosity of soil. The first, second and third terms of (4) are the vertical diffusion of water, gravity drainage and water suction by transpiration respectively. The parameters heat conductivity λ , water diffusivity D and hydraulic conductivity K_w are the functions of soil moisture, taking Clapp & Hornberger (1978) empirical relation

$$K_w = K_{sat} W^{2b+3}, \quad (5)$$

$$D = -K_{sat} \frac{\psi_s b}{\theta_s} W^{b+2}, \quad (6)$$

where ψ_s and K_{sat} refer to the saturated soil water potential and K_w , and b is an experimental constant. For the soil surface layer, $i=1$, the heat and water fluxes at the surface are equal to

$$F_T = -\lambda \left(\frac{\partial T}{\partial z} \right) = S_g (1 - \alpha_g) + R_{Lg} - \sigma T_1^4 - H_g - LE_g - L_{SN} S_N, \quad (7)$$

$$F_w = -D \cdot \left(\frac{\partial W}{\partial z} \right) = \frac{1}{\theta_s} \cdot \left[P_g - \frac{1}{\rho_w} \cdot E_g + S_N \right]. \quad (8)$$

The variables with the subscript 'g' are related to land surface. The terms on the right side of Equation (7) are short wave radiation and long wave radiation absorbed by the surface, emitted long wave radiation, sensible and latent heat fluxes and heat flux for snow melting. P_g is the precipitation: reaching directly at the surface and dropping from foliage. S_N is the melted snow amount. E_g is the surface evaporation. L is vapour latent heat and L_{SN} snow melting heat.

The sensible and latent heat fluxes (and transpiration) can be written as

$$F = \rho_a \Delta\psi / r, \quad (9)$$

where ρ_a is air density at the surface, $\Delta\psi$ the difference of transport variables and r the resistance in the transport way. In the space between soil, vegetation and the atmosphere $r = (u \cdot C_D)^{-1}$, u is the wind speed and C_D the drag coefficient, which depends on the height of plant, dynamical roughness of canopy and ground, leaf size and foliage orientation distribution as well as leaf area index and coverage (Ji, 1995). For example, the stomata resistance of canopy is:

$$r_f = r_0 (\sigma_f \cdot I_{LA})^{-1}, \quad (10)$$

where r_0 is the stomatal resistance against water for unit leaf area, I_{LA} is the leaf area index. With the plant growth the structure and morphology of vegetation vary, consequently, the physical exchange between soil, vegetation and the atmosphere also varies.

2.1.2 Physiological growth processes

The right side of system shows the physiological growth processes of vegetation (Fig. 1). Vegetation consists of three tissues: leaf, stem and root and a litter layer. The prognostic equation of biomass for each tissue is

$$\frac{dM_j}{dt} = \eta_j (1 - \sigma_j) \cdot \left[A - \sum_{j=1}^3 R_{mj} \right] - \beta_j \cdot M_j - L_{oj} \quad j = f, s, r. \quad (11)$$

The subscript 'j' denotes f, s and r standing for the variables related to leaf, stem and root respectively. M_j is the biomass, η_j the allocation coefficients of dry matter to the tissues. σ_j is the growth respiration coefficients of tissues. A is the gross photosynthetic rate. R_{mj} is the maintenance respiration rate. β_j is the falling rate of stem and leaf or the root mortality rate. L_{oj} is the consumption by animals, cutting and fire. The details of process

parameterization refer to Ji (1995, 1996).

The gross photosynthetic rate is controlled by environmental factors and leaf states, such as leaf temperature, CO₂ concentration in the stomata C_i , leaf water potential ψ_f and nitrogen concentration of leaf N

$$A = P_{\max} f(C_i) f(T_f) f(\psi_f) f(N) . \tag{12}$$

The function in (12) can be found in Ji (1995, 1996). Here P_{\max} is the canopy photosynthetic rate under the optimum conditions. Taking Michaelis-Menten form

$$P_{\max} = \frac{P_{\text{sat}}}{K} \ln \frac{P_{\text{sat}} + B \cdot I_0}{P_{\text{sat}} + B \cdot I_0 e^{-K \cdot I_{LA}}} , \tag{13}$$

where P_{sat} is the photosynthetic rate at the light saturation. B is the scope of the photosynthetic curve at the light compensation point and I_0 is the photosynthetic active radiation at the top of canopy. K is the extinction coefficient of canopy.

The photosynthetic rate identifies the CO₂ diffusive rate from the atmosphere to stomata, i.e.

$$A = (C_a - C_i) g_s / 1.6 , \tag{14}$$

where C_a is CO₂ concentration in canopy space, g_s the conductance against water, 1.6 is the ratio of conductance of water to CO₂. Because both water transpiration and CO₂ assimilation pass simultaneously leaf stomata, the experiment shows that there exists a linear relationship between stomatal conductance and photosynthetic rate (Collatz et al., 1991), substituting C_s and e_s with C_a and e_a , the modified formula is given by

$$g_s = m \cdot \frac{P_0}{C_a} \cdot r_h A + b . \tag{15}$$

Here g_s is the stomatal conductance and P_a the pressure at the surface. C_s and e_s are CO₂ concentration and vapour pressure over leaf surface and r_h is the relative humidity at the leaf temperature. m and b are the experimental constants. From (13), (14) and (15), the photosynthetic rate and stomatal conductance or resistance r_{f0} can be determined.

Both the maintenance respiration R_m and growth respiration R_g are taken into consideration in the model. The maintenance respiration depends mainly on temperature, and growth respiration is proportional to the growth rate of dry matter of tissue. They can be written as

$$R_{mi} = \alpha_i M_i Q^{0.1 \cdot (T - T_0)} \quad i = f, s, r \tag{16}$$

and

$$\begin{cases} R_{gi} = \sigma_i \eta_i (A - R_m) & A - R_m > 0 , \\ R_g = 0 & A - R_m \leq 0 , \end{cases} \tag{17}$$

where α_i is the respiration rate per unit biomass at temperature T_0 . Q is a constant (around 2). And T_0 is a reference temperature.

The falling of stem and mortality of root are assumed to be random processes, and the falling rate is related to the life time and biomass of tissue, while the falling of foliage is dependent on temperature and phenological period. The prognostic equation of dry matter of litter M_d is

$$\frac{dM_d}{dt} = \sum_{j=1,2,3} \beta_j M_j - \beta_d \cdot M_d, \quad (18)$$

where the decomposition rate β_d is a function of soil temperature and moisture.

A key variable I_{LA} can be determined from leaf biomass, which is used to calculate the physical parameters at the surface, such as canopy roughness, albedo.

2.2 Classification of vegetation and soil texture

In regard to the classification of plant functional type (PFT) on global scale, it must consider the following factors: (1) PFT must involve main vegetation types, natural vegetation and artificial vegetation, eg. crops; (2) PFT is able to express the function and feature of vegetation and (3) PFT must cover whole continents geographically (Box, 1996). In this study, a phenological physiology-structure classification method is adopted. Globally, terrestrial ecosystems are classified into 13 types, the type and its numbers of $0.5^\circ \times 0.5^\circ$ latitude-longitudinal grid cells are shown in Table 1. The data sources of vegetation are available from the vegetation classification of Dorman and Sellers (1989), and for China modified by China Vegetation Map (Editorial Board of National Atlas, 1999).

Table 1. Global vegetation types and grid cells

Index	Types	Points number
1	Tropical rainforest	5284
2	Broad leaf deciduous trees	2136
3	Broad leaf and needle leaf trees	3536
4	Needle leaf evergreen trees	8892
5	Needle leaf deciduous trees	3928
6	Broadleaf trees with ground cover	8164
7	Ground cover only	6732
8	Broadleaf shrub with ground cover	1964
9	Broadleaf shrubs with bare soil	6307
10	Dwarf trees with ground cover	9376
11	Bare soil	2660
12	Crops	6280
13	Ice	28676
0	Water	165264
Total		295200

Table 2. Global soil texture classification and grid cells

Index	Soil texture	Points number
1	Coarse	16460
2	Medium / coarse	4708
3	Medium	29902
4	Fine / medium	4464
5	Fine	8514
6	Organic	1212
0	Ice and ocean	193940
Total		295200

The main parameters used in AVIM are those related to physiological processes: photosynthesis, respiration, allocation and decomposition of dry matter and plant morphology as well as physical parameters of soil texture. All of the above parameters are designed for each vegetation type and soil texture. The physical and dynamical parameters of the surface, such as roughness, zero-plane displacement and albedo are related to time-dependent plant morphological parameters. Physiological parameters for each vegetation type refer to Larcher (1995), Melillo et al. (1993), Li (1996), and Schulze et al. (1994) etc.

The soil texture is classified into 6 types with NASA methodology on the basis of composition proportions of clay, silt and sand (Table 2). According to the empirical relations (5) and (6), the soil parameters for each type are the soil porosity, saturated water potential, saturated hydraulic conductivity, soil heat content, wilting soil moisture and a coefficient b , which can be found in Clapp and Hornberger (1978).

3. NPP simulation results

The carbon exchange between terrestrial ecosystem and the atmosphere, i.e. the net primary productivity (NPP) was simulated with AVIM. The monthly climate datasets ($0.5^\circ \times 0.5^\circ$ lat.-long.) used in the simulation are provided from CRU. Because of short integrating time step 30 minutes for physical processes, as the input, the daily datasets were generated from monthly data by a weather generator (Friend, 1998).

3.1 Model calibration for NPP

First, we calibrate the simulated NPP at a grid cell nearby the site with observed NPP at 1637 stations distributed globally, belonging to different ecosystems, namely, evergreen coniferous forest, broadleaf deciduous forest, tropic rain forest, shrub and grassland etc. (Fig. 2). From Fig. 2 we can see that the simulated NPP at the most sites fit to the observed, the correlation coefficient between them is 0.86. It is indicated that AVIM is able to simulate NPP for global terrestrial ecosystems.

3.2 Analysis of simulated NPP

The global distribution of simulated NPP is shown in Fig. 3. Generally, compared with the composite simulated NPP map given by Cramer et al. (1999), the distribution pattern of

Table 3. Distribution areas and estimated annual NPP for global vegetation types

Index	Area (10^6 km^{-2})	NPP ($\text{g C m}^{-2}\text{yr}^{-1}$)	Total NPP (Gt C yr^{-1})
1	15.89	996.82	15.84
2	5.66	617.41	3.49
3	7.56	540.73	4.09
4	14.54	345.55	5.02
5	5.88	377.42	2.22
6	23.1	586.54	13.55
7	16.1	287.79	4.63
8	5.48	486.96	2.67
9	16.84	199.16	3.35
10	9.94	99.58	0.99
11	7.05	0	0
12	15.03	323.64	4.86
Total	143.07	(average 405.13)	60.72

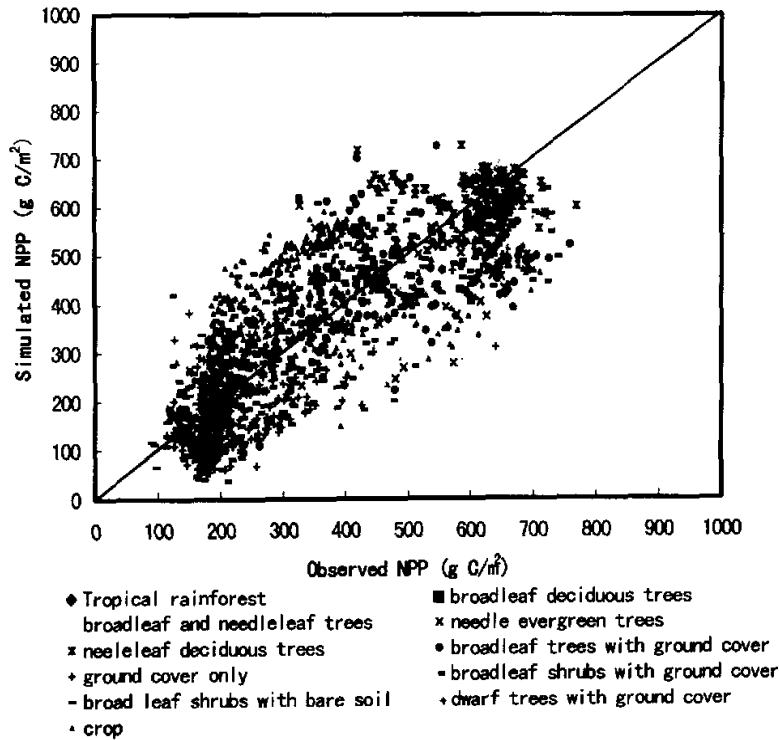


Fig. 2. Comparison of observed NPP and simulated NPP by AVIM (observed data are provided by Ecosystem Model Data Intercomparison (EMDI) project).

NPP is reasonable. For a single cell of $0.5^\circ \times 0.5^\circ$, the NPP varies in the range of $0\text{--}1800 \text{ g C m}^{-2}\text{yr}^{-1}$. For different vegetation types, the averaged NPP vary from $99.58 \text{ g C m}^{-2} \text{ yr}^{-1}$ for tundra to $996.82 \text{ g C m}^{-2}\text{yr}^{-1}$ for tropic rain forest. The global averaged NPP is about $405.13 \text{ g C m}^{-2} \text{ yr}^{-1}$ (Table 3).

3.2.1 Spatial distribution of carbon exchange

The zonal averaged NPP for each 5° lat. is displayed in Fig. 4. For NPP per unit area, the highest occurs in the tropics between $15^\circ\text{N}\text{--}15^\circ\text{S}$, where covers tropical rainforest. The maximum NPP may reach $953 \text{ g C m}^{-2}\text{yr}^{-1}$. Between $60^\circ\text{N}\text{--}30^\circ\text{N}$, Northern middle latitudes, NPP is the second high, while in the subtropics NPP is rather low because of relatively dry climate. For total amount of NPP in a latitude zone, the largest one is in the Northern middle latitudes, where vegetation coverage area is the largest, the second is in the Northern temperate zone, the annual total NPP for 0.5° latitude zone reaches 0.8 Gt C . The annual NPP in the latitude zone between $60^\circ\text{N}\text{--}30^\circ\text{N}$ account for 44.0 % of global total terrestrial ecosystem NPP, 22.7% in tropical zone $15^\circ\text{N}\text{--}15^\circ\text{S}$ and 11.1% in the Southern middle-low latitude zone $15^\circ\text{S}\text{--}60^\circ\text{S}$. The latitudinal distribution of simulated NPP by AVIM agrees with the results reported by Cao and Woodward (1998) and Cramer et al. (1999).

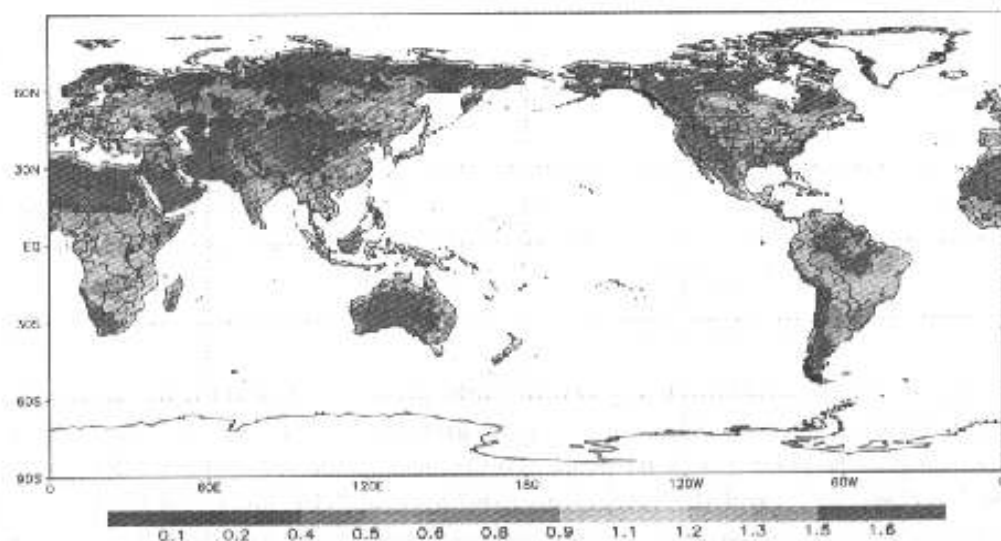
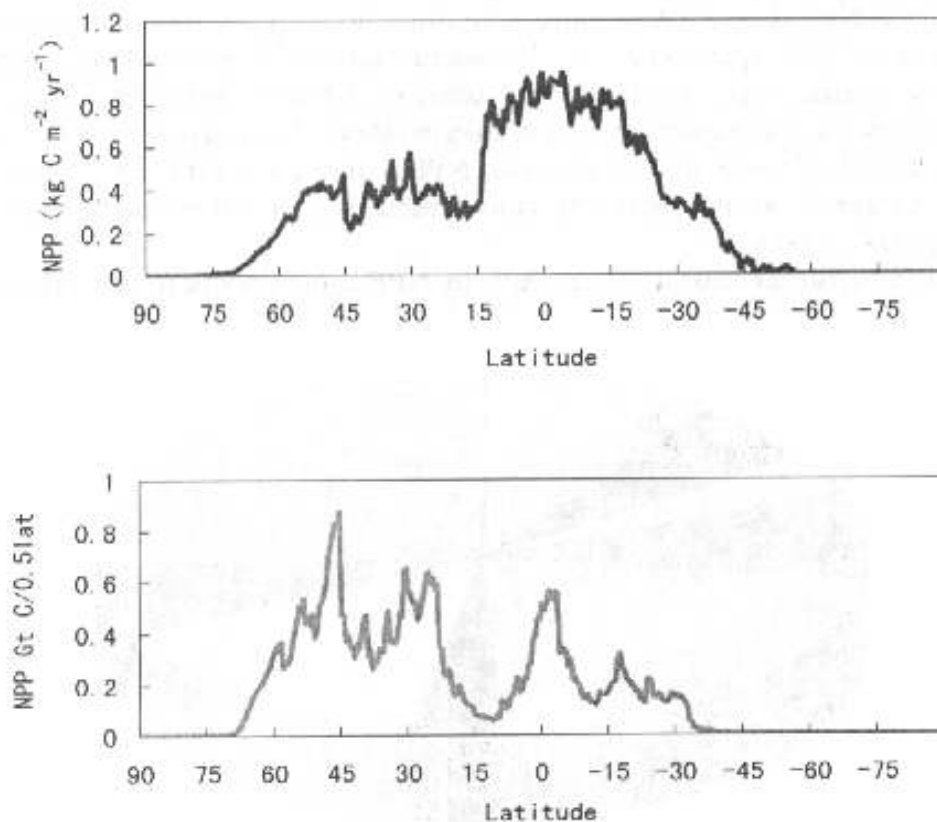
Annual NPP of global terrestrial ecosystem (kg C/m^2)Fig. 3. Global terrestrial ecosystem annual NPP distribution (Unit: kg C/m^2).

Fig. 4. Latitudinal distribution of specific area NPP (top) and total NPP (bottom).

For China, the simulated NPP is significantly controlled by thermal and humid climatic conditions, showing the decreasing trends from southeast to northeast. In Southeast China, the maximum NPP may reach $1000 \text{ g C m}^{-2} \text{ yr}^{-1}$. Around the middle and lower reaches of the Yangtze River, NPP is about $500 \text{ g C m}^{-2} \text{ yr}^{-1}$. While over the western highland and arid/semiarid regions NPP is less than $100 \text{ g C m}^{-2} \text{ yr}^{-1}$. These results are consistent with those obtained by the empirical model of Zhou and Zhang (1996) and the satellite remote sensing model of Sun and Zhu (2000).

Recently the global annual NPPs are simulated by 13 models participating the comparison project (PIK), which are in the range of $39.9\text{--}80.5 \text{ Gt C yr}^{-1}$ with on the average of $54.9 \text{ Gt C yr}^{-1}$. The global annual NPP in this study is about $60.72 \text{ Gt C yr}^{-1}$, which is slightly higher than the averaged of 13 models.

3.2.1 NPP for different vegetation types

The coverage area for different vegetation types are quite different, in which, the maximum 23.1 Mkm^2 is covered by broadleaf forest, and the second 15.89 Mkm^2 by tropical rainforest. Among vegetation types tropical rainforest has the maximum NPP for per unit area i.e. $996.2 \text{ g C m}^{-2} \text{ yr}^{-1}$, and the maximum total annual NPP i.e. $15.84 \text{ Gt C yr}^{-1}$. Therefore tropical rainforest is a main carbon sink, playing an important role in the absorption of CO_2 in the atmosphere (Philips et al. 1998). But heterotropical respiration of soil in tropical regions is also high (Nemry et al. 1999), this would reduce the role of carbon sink. The second and third total annual NPPs belong to broad leaf forest with ground cover and evergreen coniferous forest, respectively. The total NPP of these vegetation types accounts for about 56% of global annual NPP (Fig. 5). Associated with other forest types, the total annual NPP for forest accounts for 80% approximately. Thus we can say that forest is a lump of the earth, it means forest is capable largely to absorb and exchange carbon with the atmosphere.

Grassland is also an important terrestrial ecosystems, its coverage areas is slightly less than that of broadleaf forest, and total annual NPP is about $4.63 \text{ Gt C yr}^{-1}$. Grassland associated with savannah would show the considerable role in terrestrial carbon exchange (Scurlock and Hall, 1998).

Crops is the artificial ecosystem, generally its NPP approximates to natural ecosystem in

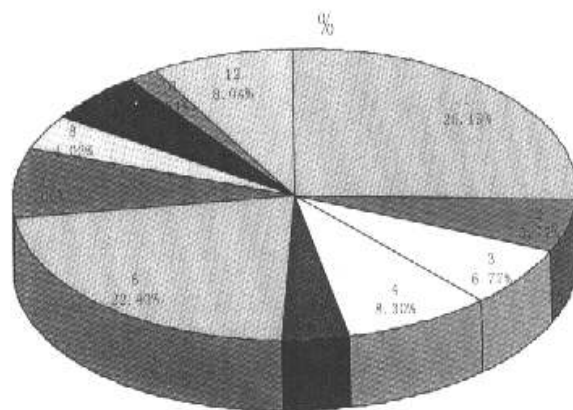


Fig. 5. Percentage of different vegetation types NPP in the global total.

the same region. In this study, the simulated total NPP of crops is about 4.86 Gt C yr⁻¹.

4. Conclusions and discussion

In this study, the carbon exchange between ecosystem and the atmosphere (NPP) was simulated with the Atmosphere-Vegetation Interaction Model (AVIM), and global distribution of NPP and its latitudinal variation are also analysed. The conclusions can be drawn as follows.

- (1) By calibration of modelled NPP for different vegetation types it is indicated that AVIM is capable of simulating NPP globally. The structure of AVIM and the parameters for each vegetation type and soil texture used in AVIM are feasible and efficient.
- (2) The global averaged NPP of terrestrial ecosystem simulated by AVIM is about 405.13 g C m⁻²yr⁻¹. For different ecosystems, NPP per unit area varies from the lower value 99.58 g C m⁻²yr⁻¹ for tundra to the higher 996.82 g C m⁻²yr⁻¹ for tropical rainforest.
- (3) The global total NPP is estimated to be 60.72 Gt C yr⁻¹, which is in the varying range of estimates by 13 ecosystem models of international comparison project. The total NPP for tropical rainforest is the highest among different ecosystems, accounting for 26.09% of the global totals. The second and third larger amounts belong to broadleaf forest and evergreen coniferous forest.

The carbon flux between vegetation and the atmosphere is an important issue in global change, and needs to be investigated furthermore. This study is a preliminary result of NPP simulation. The Ecosystem Model / Data Intercomparison (EMDI) project launched recently provides a possibility of validating and improving the ecosystem model, and to studying the carbon cycles in the earth system further.

REFERENCES

- Bonan, G. B., 1996: A Land Surface Model (LSM 1.0) for ecological, hydrological and atmospheric studies: Technical description and users guide. NCAR / TN-417+STR.
- Box, E. O., 1996: Plant functional types and climate at the global scale. *Journal of Vegetation Science*, **7**, 309-320.
- Cao, M., and F. I. Woodward, 1998: Net primary and ecosystem production and carbon stocks of terrestrial ecosystems and their responses to climate change. *Global Change Biology*, **4**, 185-198.
- Clapp, R. B., and G. M. Hornberger, 1978: Empirical equations for some soil hydraulic properties. *Water Resources Research*, **14**(4), 601-604.
- Collatz, G. J., J. T. Ball, C. Grivet, et al., 1991: Physiological and environmental regulation of stomatal conductance, photosynthesis and transpiration: a model that includes a laminar boundary layer. *Agricultural and Forest Meteorology*, **54**, 107-136.
- Cramer, W., D. W. Kicklighter, A. Bondeau, et al., 1999: Comparing global models of terrestrial net primary productivity (NPP): overview and key results. *Global Change Biology*, **5** (suppl.1), 1-5.
- Dorman, J. L., and P. J. Sellers, 1989: A global climatology of albedo, roughness length and stomatal resistance for atmospheric general circulation model as represented by the simple biosphere model. *Journal of Applied Meteorology*, **28**, 833-855.
- Editorial Board of National Atlas, 1999: *National Natural Atlas of People's Republic of China*, Beijing: China Atlas Press 283pp.
- Friend, A. D., 1998: Parameterisation of a global weather generator for terrestrial ecosystem modelling. *Ecological Modelling*, **109**, 121-140.
- IPCC (Intergovernmental Panel on Climate Change), 2001: Summary for Policymakers (SPM) and Technical Summary. From www.ipcc.ch/pub/.

- Ji Jinjun, and Hu Yuchun, 1989: A simple land surface process model for use in climate study. *Acta Meteorologica Sinica*, **3**, 344–353.
- Ji Jinjun, and Hu Yuchun, 1999: A multi-level canopy including physical transfer and physiological growth processes. *Climatic and Environmental Research*, **4**(2), 152–164 (in Chinese).
- Ji Jinjun, and Yu Li, 1999: A simulation study of coupled feedback mechanism between physical and biogeochemical processes at the surface. *Chinese Journal of Atmospheric Sciences*, **23**(4), 439–448 (in Chinese).
- Ji, J., 1995: A climate-vegetation interaction model: simulating physical and biological processes at the surface. *Journal of Biogeography*, **22**, 445–451.
- Larcher W., 1995: *Physiological Plant Ecology* (3rd ED). Germany: Springer-Verbeget 506pp.
- Li Wenhua and Li Fei, 1996: *Study on Forest Resources of China*. Beijing: China Forestry Press 336pp.
- Lieth H., 1975: Modeling the primary production of the world. In: *Primary Productivity of the Biosphere* (eds. Lieth and Whittaker), Berlin: Springer-Verlag 339pp.
- Lu Jianhua, 1999: A simulation study of regional atmosphere-vegetation interactions on seasonal and interannual scales, Ph. D. dissertation, Institute of Atmospheric Physics, Chinese Academy of Sciences (in Chinese).
- Melillo, J. M., A. D. McGuire, D. W. Kicklight et al., 1993: Global climate change and terrestrial net primary production. *Nature*, **363**, 234–240.
- Nemry B., L. Francois, J-C Gerard et al., 1999: Comparing global models of terrestrial net primary productivity (NPP): Analysis of the seasonal atmospheric CO₂ signal. *Global Change Biology*, **5**(suppl. 1), 65–76.
- Philips, O. L., Y. Malhi, N. Higuchi et al., 1998: Changes in carbon balance of tropical forests: Evidence from long-term plots. *Science*, **282**, 442–446.
- Sahagian D., 2000: Highlight of GAIM's first phase: Building towards earth system science. *Global Change Newsletter*, **41**(May), 11–15.
- Schulze, E. D., F. M. Kelliher, J. Lloyd et al., 1994: Relationship among maximum stomatal conductance, ecosystem surface conductance, carbon assimilation rate, and plant nitrogen nutrition: A global ecology scaling exercise. *Annu. Rev. Ecol. Syst.*, **25**, 629–660.
- Scurlock JMO, and D. O. Hall, 1998: The global carbon sink: A grassland perspective. *Global Change Biology*, **4**, 229–233.
- Sun Rui, and Zhu Qijiang, 2000: Distribution and seasonal change of net primary productivity in China from April, 1992 to March, 1993. *Acta Geographica Sinica*, **55**(1), 36–45 (in Chinese).
- Zhou Guangsheng, and Zhang Xinshi, 1996: Study on NPP of natural vegetation in China under global climate change. *Acta Phytocologica Sinica*, **20**(1), 11–19 (in Chinese).

全球植被与大气之间碳通量的模式估计

李银鹏 季劲钧

摘 要

用大气植被相互作用模式(AVIM)模拟了全球陆地植被的净初级生产力(NPP)。AVIM由相互耦合的两部分组成:物理过程,包括陆地表面水分和能量在土壤、植被与大气之间的传输;以及生理生态过程,如:光合、呼吸、干物质分配、凋落和物候等。全球的植被分为13类,土壤按质地分为6类。用EMDI提供的全球1637个包括不同植被类型的NPP观测点数据对模型进行了检验。NPP模拟的结果表明:全球陆地植被的平均NPP为 $405.13 \text{ g C m}^{-2} \text{ yr}^{-1}$,不同植被类型的平均NPP变化范围在 $99.58 \text{ g C m}^{-2} \text{ yr}^{-1}$ (苔原)到 $996.2 \text{ g C m}^{-2} \text{ yr}^{-1}$ (热带雨林)之间。全球年总NPP为 $60.72 \text{ Gt C yr}^{-1}$,其中最大的部分为热带雨林, $15.84 \text{ Gt C yr}^{-1}$,占全球的26.09%。最大的碳汇是在北半球的温带。模式模拟的NPP在全球的空间和季节分布是合理的。

关键词: 碳通量, 净初级生产力(NPP), 陆地生态系统, 大气植被相互作用